Title	Numerical reconstruction of high dose rate zones due to the Fukushima Dai-ichi Nuclear Power Plant accident
Author(s)	Genki Katata, Hiroaki Terada, Haruyasu Nagai, Masamichi Chino
Citation	Journal of Environmental Radioactivity, 111 ; p.2-12
Text Version	Author
URL	http://jolissrch-inter.tokai-sc.jaea.go.jp/search/servlet/search?5031094
DOI	http://dx.doi.org/10.1016/j.jenvrad.2011.09.011
Right	This is the author's version of a work that was accepted for publication in < Journal of Environmental Radioactivity>. Changes resulting from the publishing process, such as peer review, editing, corrections, structural formatting, and other quality control mechanisms, may not be reflected in this document. Changes may have been made to this work since it was submitted for publication. A definitive version was subsequently published in Journal of Environmental Radioactivity,, vol.111, p.2-12(Sep. 2012), http://dx.doi.org/10.1016/j.jenvrad.2011.09.011.

Numerical reconstruction of high dose rate zones due to the Fukushima Daiichi Nuclear Power Plant accident

Keywords: Fukushima Daiichi Nuclear Power Plant accident; atmospheric dispersion; surface deposition; high dose rate zones; numerical simulation; WSPEEDI-II

Abstract:

To understand how the high dose rate zones created during the Fukushima Daiichi Nuclear Power Plant (FNPP1) accident on March 2011, the atmospheric dispersion of radionuclides during the period from 15 to 17 March was reproduced by using a computer-based nuclear emergency response system, WSPEEDI-II. With use of limited environmental monitoring data, prediction accuracy of meteorological and radiological fields by the system was improved to obtain best estimates of release rates, radiation dose maps, and plume movements. A large part of current high dose rate zones in Fukushima was explained by simulated surface deposition of radionuclides due to major releases of radionuclides on 15 March. In the simulation, the highest dose rate zones to the northwest of FNPP1 were created by a significant deposition of radionuclides discharged from FNPP1 during the afternoon. The results indicate that two environmental factors, i.e., rainfall and topography, strongly affected the spatial patterns of surface deposition of radionuclides. The wet deposition due to rainfall particularly played an important role in the formation of wide and heterogeneous distributions of high dose rate zones. The simulation also demonstrated that the radioactive plume flowed along the valleys to its leeward, which can expand the areas of a large amount of surface deposition in complex topography.

1. Introduction

In the Fukushima Daiichi Nuclear Power Plant (hereinafter referred to as FNPP1) accident, it was clarified by aerial and ground-level radiation monitoring (MEXT and DOE, 2011) carried out after 16 March (Fig. 1a, reproduced by the authors) that the high dose rate zones had been formed to the northwest direction from FNPP1. It is important to understand how these zones were created for radiological dose assessment for the accident. The key of its formation is considered to be a significant release of radionuclides (such as ^{131}I and ^{137}Cs) that can be deposited onto the ground surface on 15 March, 2011 estimated by Japan Atomic Energy Agency (JAEA). The preliminary estimation of the release rates of radionuclides indicates that the zones were formed due to a significant release on 15 March, 2011 (Chino et al. 2011). At 9 Japan Standard Time (JST = UTC + 9 h) on 15 March, air dose rate at the main gate of FNPP1 rapidly increased up to approximately 12 mGy h^{-1} after an explosive sound around the suppression chamber of Unit 2 at 6:10 JST (TEPCO, 2011a). Then, air dose rates rose up at several off-site monitoring posts (Kawauchi, Koriyama, Iitate, and Fukushima) located at the southwest to north directions of FNPP1 in turn until the midnight (Fig. 1b). The highest value of air dose rate of 44.7 μGy h^{-1} was observed at 18:20 JST at the monitoring post in Iitate (Fukushima Prefecture, 2011a) located 40 km northwest of FNPP1. These data imply that the radioactive plume changed its flow direction clockwise and passed through monitoring posts in various directions.

Figure 1

The formation process of high dose rate zones can be normally investigated by analyzing environmental observation data such as meteorological condition, radiation dose, concentration and deposition of radionuclides. However, some important equipment (e.g., stack monitors, radiation and meteorological stations), which was deployed within 20 km from FNPP1 to measure air dose rates and meteorological conditions, did not work on 15 March, 2011 due to the severe earthquake and/or tsunami. Consequently, it was difficult to analyze in detail how the plume flowed from FNPP1 and formed the high dose rate zones. To reveal the formation mechanism further, numerical simulation of the event of atmospheric dispersion on 15 March, 2011 is required.

In the present paper, we tried to reconstruct the event on 15 March by coupling limited environmental data with numerical simulations of computer-based nuclear emergency response system, WSPEEDI-II (Terada et al., 2008). The reconstruction was carried out by two successive ways. The first is the estimation of temporal changes in release rates on 15 March by comparing air dose rates calculated under the assumption of unit release rate (1 Bq h^{-1}) with observed one. The second is the elucidation of formation process of high dose rate zones based on the transport, diffusion and deposition on the ground surface of plumes reproduced in the simulation.

2. Methodology

2.1. Study area and the environmental data

Three computational domains are set for meteorological prediction and inner two domains are used for atmospheric dispersion calculation (Fig. 2). The area for comparison with the measurements is 190-km square area in Fukushima Prefecture, Japan. The site of FNPP1 is located near the Pacific coast and lies on the East side of Abukuma highland with an altitude up to 1000 m. Meteorological data of wind and air temperature and humidity observed at surface weather stations around FNPP1 (Figs. 3 and 4) were used for data assimilation of MM5. In addition, the data of wind speed and direction at the ground surface at FNPP1 and at the top of stack with 120 m height at Fukushima Daini nuclear plant (hereinafter referred to as FNPP2, METI, 2011; Fig. 5) were used to correct wind fields around the plant. To estimate the release rates and to validate the simulation results, we used the data of airborne (MEXT and DOE, 2011; DOE, 2011) and ground-level monitoring in Fukushima (Fukushima Prefecture, 2011a and b; TEPCO, 2011b), Ibaraki (Ibaraki Prefecture, 2011; Ibaraki Prefectural Environmental Radiation Monitoring Center, 2011; JAEA, 2011), and Tochigi Prefectures (Tochigi Prefecture, 2011).

Figure 2

Figure 3

Figure 4

Figure 5

2.2. Radionuclides

In our calculations, the major radioactive species of ^{131}I, ^{132}I, ^{132}Te, ^{134}Cs, and ^{137}Cs

were considered to be discharged from FNPP1. Iodine-132 is treated as ^{132}Te progeny nuclide and radioactive equilibrium between ^{132}Te (half-life = 3.2 d) and ^{132}I (half-life = 2.3 h) is assumed. Thus, in our simulation, ^{132}I and ^{132}Te discharged into the atmosphere have the same radioactivity and half-life. The radioactivity ratio ^{131}I:(^{132}I+^{132}Te):^{134}Cs:^{137}Cs was set to be 1:2:0.1:0.1 based on that the ratio of ^{131}I to other nuclides derived from measured airborne concentrations at Tsukuba (KEK, 2011). Radioactive noble gas, ^{133}Xe (half-life = 5.2 d), was not considered in this paper since the study mainly focuses on atmospheric movements of radionuclides that can be deposited onto the ground surface. Such approach may lead to a discrepancy of air dose rate between calculation and measurement for the period of the passage of plume. By considering this effect of ^{133}Xe, the monitoring data during the plume passage were used to investigate the movements of plume. The simulated air dose rates were quantitatively compared with observed ones due to ground-shines of deposited radionuclides after the plume passed away (see Section 2.4).

2.3. Models

The computer-based nuclear emergency response system, Worldwide Version of System for Prediction of Environmental Emergency Dose Information (WSPEEDI-II) was used to reproduce the event which had occurred in the atmospheric environment during the period from 15 to 17 March 2011 in Fukushima Prefecture, Japan (Fig. 2). WSPEEDI-II includes the combination of models, a non-hydrostatic atmospheric dynamic model (MM5, Grell et al., 1994) and Lagrangian particle dispersion model (GEARN, Terada and Chino 2008). MM5 predicts three-dimensional fields on wind, precipitation, diffusion coefficients, etc. based on atmospheric dynamic equations with appropriate spatial and temporal resolution, by using domain nesting method. GEARN calculates the advection and diffusion of radioactive plumes, dry and wet deposition onto the ground surface, and air dose rate from radionuclides in the air by the submersion model and on the ground surface (ground-shine). GEARN can predict the atmospheric dispersion for two domain simultaneously based on the meteorological fields of each domain by MM5 by considering in- and outflow between the domains. The performance of this model system was evaluated by its application to the field tracer experiment over Europe, ETEX (Furuno et al., 2004) and Chernobyl nuclear accident (Terada et al. 2004; Terada and Chino 2005, 2008). Further information of WSPEEDI-II is available in Terada et al. (2004) and Terada and Chino (2005). The simulation conditions of MM5 and GEARN are summarized in Tables 1 and 2, respectively.

Table 1

Table 2

Concerning deposition processes in GEARN, deposition velocity is set to typical value for short vegetation, such as grassland (Sehmel, 1980). However, it is known that dry deposition velocity is larger for forest than that for grass (Sportisse, 2007) because forests have tall canopy height and large leaf surface area that enable to capture a large amount of radionuclides in the atmosphere. To roughly simulate this effect, GEARN was modified to use five times larger deposition velocity at the grids with forest category in MM5 than that used at other categories.

2.4. Reconstruction process of atmospheric dispersion

Reconstruction procedure in the present study is summarized in Fig. 6. Firstly, meteorological fields were reproduced by using a four-dimensional data assimilation method to nudge prediction results by MM5 to observed meteorological data at FNPP1, FNPP2, and surface weather stations in Fukushima Prefecture. Then, based on the reproduced meteorological fields, GEARN was used to simulate atmospheric dispersion and radiological events during the period from 15 to 17 March by using preliminary estimated release rates by Chino et al. (2011). The detailed release rates were estimated by that calculated air dose rates along or not along the passage of plumes due to ground-shines (see Fig. 1b) were consistent with those from observations at monitoring posts. Prediction accuracy of GEARN was mainly evaluated by comparisons of air dose rate at Fukushima, Iitate, Koriyama, Tamura, Kawauchi, and Minamisoma in Fukushima Prefecture (Fukushima Prefecture, 2011a and b) between calculations and measurements (Fig. 7) using the statistical indicator of percentage of the calculated values within factors to the measurements. In addition, the spatial distributions of air dose rate calculated by GEARN were also compared with aerial measurements (Fig. 1a, MEXT and DOE, 2011). When there discrepancies of the amount and temporal variation of air dose rates at monitoring points between simulations and measurements were significant, the release rates and durations were modified for recalculation by GEARN.

Figure 6

Figure 7

The revision was extended to the correction method of meteorological field in MM5 simulation (Figs. 3, 4, and 5), when the discrepancy of distribution patterns of air dose rates appeared. Figures 3–5 show the comparisons between calculations and observations for wind and rainfall at FNPP1, FNPP2, and the surface weather stations in Fukushima Prefecture. At FNPP1 and FNPP2 (Fig. 5), for example, the changes from easterly to southeasterly wind delayed several hours in calculations compared with observations without the analysis and observational nudging functioned in MM5. Calculated wind speed was also clearly higher than the observed one from 9 to 21 JST on 15 March. After the four-dimensional data assimilation of analysis and observation nudging were made, model predictions of wind direction and speed clearly improved, particularly in the period from 9 to 21 JST on 15 March. Tuning parameters for four-dimensional assimilation in MM5 are given in Table 1. The above procedure for meteorological and atmospheric dispersion simulations was repeated until the simulation results of air dose rate became consistent with most of the measurements.

3. Results and Discussion

3.1. Reconstructed atmospheric dispersion on 15 March, 2011

The detailed release rates on 15 March (Table 2) were determined from the comparison of temporal variations of air dose rates between calculations and observations at three monitoring posts (see Section 2.4). The accuracy of estimated release rates is considered to be within the factor 2 based on the comparisons of air dose rates between calculations and observations for six monitoring posts at 18 JST on March 16 (Fig. 7). The estimation showed two major releases of radionuclides around 7 to 10 (3.0×10^{15} Bq h^{-1} for ^{131}I) and 13 to 17 JST (4.0×10^{15} Bq h^{-1} for ^{131}I) on 15 March. The former release was also detected as the increase of air dose rate during the same period by the monitoring car at the main gate of FNPP1, while the latter was not clearly detected because the plume flowed toward the different direction from the gate. However, the rapid decreases of reactor pressure of Unit 2 of FNPP1 from 7:20 to 11:42 and from 13:00 to 16:10 JST (TEPCO, 2011c) indicate the both releases.

By using estimated release rates in the calculations, best estimates of radiation dose maps and plume movements during the period from 15 to 17 March (Fig. 8 and 9, Movie 1 and 2 available online) were obtained. In the simulation, the high dose rate zones was found to spread mainly to the northwest direction from FNPP1 (Fig. 9e), while the some discrepancies between calculation and observation appeared in overestimations of air dose rates in the north and middle parts of Fukushima. This pattern corresponded to airborne observations carried out on 17–19 March, 2011 (DOE, 2011). Time series of calculated air dose rate also agreed well with measurements at six off-site monitoring posts that included three monitoring posts used for reconstruction (Fig. 7).

Figure 8

Figure 9

Movie 1

Movie 2

Based on simulated vertically accumulated concentrations of ^{131}I, precipitation and surface wind (Figs. 8 and 9), the formation process of the high dose rate zones (Fig. 9e) is explained as follows. Increases in air dose rates at the monitoring posts at the southwest and west directions (Kawauchi and Koriyama, respectively) of FNPP1 were caused by the high-concentration plume released in the morning (7–10 JST). As shown in Figs. 8b and d, the plume represented by concentration contours of radionuclides distributed in the southwest direction of FNPP1 around 11 JST. At 14 JST, the plume encountered the rainband that covered the west and central areas, and caused some amounts of wet deposition around Koriyama (Figs. 8e and f). In the afternoon, easterly and southeasterly winds (Fig. 8f) carried the plume discharged from 13 to 17 JST to the northwest of FNPP1 (Fig. 9b). The rainfall which widely covered in the north part of Fukushima scavenged this high-concentration plume, and produced a significant amount of surface deposition and high dose rate zones at the northwest region of FNPP1 in the evening (Figs. 9a, c, e).

The circles in right panels of Figs. 8 and 9 show air dose rates at the off-site monitoring posts. Air dose rates rose up when the plume covered the posts and, even after the passage of plume, higher levels of air dose rates continued than those before the passage of plume. This fact means that radionuclides depositing on the ground surface maintain the high dose rate zones due to ground-shines (Fig. 1b).

3.2. Influences of deposition processes

To quantify the contribution of dry and wet deposition processes on air dose rates, the spatial distributions of them accumulated in the simulation period were compared (Fig. 10). Dry deposition (Fig. 10a) was clearly dominant in the southwest region of FNPP1 where no rainfall area appeared during the passage of plume. It gradually decreased with distance from FNPP1, i.e., with the decrease of ground-level concentration due to atmospheric dispersion. In contrast, wet deposition dominated the high dose rate zones in the northwest region of FNPP1 and the middle area of Fukushima Prefecture (Fig. 10b). The characteristics of wet deposition were firstly the distribution pattern was heterogeneous reflecting overlap zones of rainfall and plume and, secondary, a large amount of deposition appeared in far regions, compared with dry deposition. In fact, air dose rate from the ground-shine at Koriyama located 58 km west from FNPP1 was affected by wet deposition and became larger than that at Kawauchi, positioned 22 km west-southwest of FNPP1 (Fig. 9e). These results indicate that the dry deposition contributes to the formation of high dose rate zones close to the release point along the passage of plume and the wet deposition due to rainfall plays an important role in the formation of wide and heterogeneous high dose rate zones. It corresponds to the prior observational study on the Chernobyl nuclear accident addressing that the geographic pattern of deposited ^{137}Cs was closely related to that of rainfall (Clark and Smith, 1988).

Figure 10

3.3. Roles of rainfall and topography in spatial distributions in dose rate

Although simulated and measured air dose rates are, in general, high in the northwest region of FNPP1 (Fig. 9e), the low dose rate area mainly spreads by mountain ridge lying from the south to the north between Iitate and Fukushima. This pattern is similar to the airborne observations (Fig. 1a). Since the spatial distribution of dose rate reflects that of wet deposition (Fig. 10b), the precipitation and air concentration of radionuclides are considered to be important in the formation of such a heterogeneous pattern in air dose rate. In our simulation, rainfall covered over the north part of Fukushima Prefecture when the high-concentration plume flowed on the southeasterly wind (Fig. 9b). The rainband spread over a whole area of northwest

Fukushima Prefecture in the midnight on March 15 (Fig. 9d). However, while the high-concentration plume flowed to the northwest direction from FNPP1, accumulated precipitation was relatively small around the mountain ridges above the height of 520 m between Fukushima and Iitate (Fig. 10c). This implies that one of possible formation mechanisms of the heterogeneous pattern in air dose rate was the areal difference of rainfall occurrence.

To understand the condition of the plume when the rainfall occurred in the evening and nighttime on March 15, the relationship between topography and dry deposition (Fig. 10a) which reflects the passage of the plume at the ground level was investigated. The areas of a large amount of dry deposition, to a large extent, distributed to the northwest direction from FNPP1. However, around the location of 37°36'N and 140°48'E, the plume was divided into two branches to the west-northwest and northwest directions (Fig. 10a). The branches were located along the valleys below the altitude of 520 m. Dry deposition was relatively high at the places, compared with that in the west region from the bifurcation point of the plume. Therefore, it is likely that the high-concentration plume which mainly spread along the valleys caused the heterogeneous patterns of wet deposition and air dose rate (Fig. 10a, Movies 1 and 2). The results also indicate that, when a valley leads to the leeward of the plume, it can flow along the valley and disperse to different directions from wind. This can expand the areas of a significant amount of surface deposition of radionuclides in complex topography. The role of topography in atmospheric dispersion is supported by airborne measurements that the highest dose rate zone mainly distributes over lowland areas below a height of 520 m, which included two valleys toward the Fukushima and Iitate (Fig. 1a; MEXT and DOE, 2011).

4. Conclusions

The atmospheric dispersion of radionuclides during the period from 15 to 17 March in the Fukushima Daiichi Nuclear Power Plant accident was reconstructed by coupling environmental data with numerical simulations of computer-based nuclear emergency response system, WSPEEDI-II. Temporal changes in release rates on 15 March was estimated by comparing air dose rates calculated under the assumption of unit release rate (1 Bq h^{-1}) with observed one. By using estimated release rates, the spatial distributions and time series of observed air dose rate were overall reproduced by WSPEEDI-II. Two major releases of radionuclides in the morning and afternoon on 15 March were indicated by the numerical simulation.

A large part of current high dose rate zones in Fukushima was explained based on interactions between the deposition processes and geographical factors. The simulation results indicate that a significant amount of surface deposition was produced at the northwest region of FNPP1 in the evening when the high-concentration plume discharged in the afternoon was scavenged by rainfall. The wet deposition due to rainfall played an important role in the formation of wide and heterogeneous high dose rate zones, while the dry deposition contributed to the formation of the zones close to the release point along the passage of plume. The simulation also suggested that the plume flowed and widely dispersed along the valley that leads to its leeward and expanded the areas of a large amount of surface deposition.

Acknowledgements

The authors wish to express their gratitude to Drs. M. Ota, J. Koarashi, H. Nakayama, C. Nakanishi, A. Furuno, and S. Makimoto of Japan Atomic Energy Agency, for their helpful comments and support to partially prepare the data of air dose rates in Fukushima Prefecture. We would also like to thank the Center for Computational Science and e-Systems (CCSE) in JAEA for their support to provide the resources of supercomputer systems in JAEA. Input data for WSPEEDI-II were provided from a Meso-scale model Grid Point Value (MSM) by the Japan Meteorological Agency (JMA).

References

Chino, M., et al., 2011. Preliminary estimation of release amounts of ^{131}I and ^{137}Cs accidentally discharged from the Fukushima Daiichi nuclear power plant into atmosphere. J. Nucl. Sci. Technol. 48, 1129-1134.

Clark, M.J., and F.B. Smith, 1988. Wet and dry deposition of Chernobyl releases. Nature, 332, 245-249.

DOE, 2011. Aerial Measuring System in the United States, Radiation Monitoring Data from Fukushima Area 03/25/2011 <http://www.slideshare.net/energy/radiation-monitoring-data-from-fukushima-area-03252011> (accessed 21 July 2011).

Fukushima Prefecture, 2011a. <http://www.pref.fukushima.jp/j/20-50km0315-0331.pdf> (accessed 21 July 2011).

Fukushima Prefecture, 2011b. <http://www.pref.fukushima.jp/j/7houbu0311-0331.pdf> (accessed 21 July 2011).

Furuno, A., Terada, H., Chino, M., Yamazawa, H., 2004. Experimental verification for real-time environmental emergency response system: WSPEEDI by European tracer experiment. Atmos. Environ. 38, 6989-6998.

Grell, G.A., Dudhia, J., Stauffer, D.R., 1994. A description of the fifth-generation Penn State/NCAR Mesoscale Model (MM5). NCAR Tech. Note NCAR/TN-3921STR, 122 pp.

Ibaraki Prefecture, 2011. <http://www.pref.ibaraki.jp/20110311eq/radiation.html> (accessed 21 July 2011).

Ibaraki Prefectural Environmental Radiation Monitoring Center, 2011. <http://www.houshasen-pref-ibaraki.jp/earthquake/doserate_past.html> (accessed 21 July 2011).

Japan Atomic Energy Agency (JAEA), 2011. Transition of radiation rates measured at environmental monitoring posts of the sites of JAEA <http://www.jaea.go.jp/english/jishin/e-monitor.pdf> (accessed 21 July 2011).

KEK, High Energy Accelerator Research Organization, 2011. Measurement result of airborne nuclide and air radiation level in Tsukuba area <http://www.kek.jp/quake/radmonitor/index-e.html> (accessed 21 July 2011).

Ministry of Economy, Trade and Industry (METI), 2011. <http://www.meti.go.jp/press/ 20110316001/20110316001-2.pdf > (accessed 21 July 2011).

Ministry of Education, Culture, Sports Science and Technology (MEXT) and U. S. Department of Energy (DOE), 2011. MEXT and DOE Airborne Monitoring <http://www.mext.go.jp/english/incident/1304796.htm> (accessed 22 July 2011).

Sehmel, G.A., 1980. Particle resuspension: A review. Environ. Int. 4, 107-127.

Sportisse, B., 2007. A review of parameterizations for modelling dry deposition and scavenging of radionuclides. Atmos. Environ., 41, 2683-2698.

Tokyo Electric Power Company (TEPCO), 2011a. Radiation dose measured in the Fukushima Daiichi Nuclear Power Station <http://www.tepco.co.jp/en/nu/fukushima-np/f1/index-e.html> (accessed 21 July 2011).

TEPCO, 2011b. Radiation dose measured in the Fukushima Daini Nuclear Power Station <http://www.tepco.co.jp/en/nu/fukushima-np/f2/index-e.html> (accessed 21 July 2011).

TEPCO, 2011c. The parameters related to the plants in Fukushima Daiichi Nuclear Power Station <http://www.tepco.co.jp/en/nu/fukushima-np/index-e.html> (accessed 21 July 2011).

Terada, H., Chino, M., 2005. Improvement of Worldwide Version of System for Prediction of Environmental Emergency Dose Information (WSPEEDI), (II) Evaluation of numerical models by ^{137}Cs deposition due to the Chernobyl nuclear accident. J. Nucl. Sci. Technol. 42, 651-660.

Terada, H., Chino, M., 2008. Development of an atmospheric dispersion model for accidental discharge of radionuclides with the function of simultaneous prediction for multiple domains and its evaluation by application to the Chernobyl nuclear accident. J. Nucl. Sci. Technol. 45, 920-931.

Terada, H., Furuno, A., Chino, M., 2004. Improvement of Worldwide Version of System for Prediction of Environmental Emergency Dose Information (WSPEEDI), (I) New combination of models, atmospheric dynamic model MM5 and particle random walk model GEARN-new. J. Nucl. Sci. Technol. 41, 632-640.

Terada, H., et al., 2008. Development of Worldwide version of system for prediction of environmental emergency dose information: WSPEEDI 2nd version. Trans. At. Energy Soc. Japan. 7, 257-267 (in Japanese with English abstract).

Tochigi Prefecture, 2011. <http://www.pref.tochigi.lg.jp/kinkyu/documents/20110312-18.pdf > (accessed 21 July 2011).

Movie 1 The movie shows the computed atmospheric dispersion of radionuclides during the period from 15 to 17 March, 2011. Grey and black colored cloud in the air represent the surface of three-dimensional ^{131}I concentration with the specific levels 10^4 and 3×10^5 Bq m^{-3}, respectively. Color shaded areas at the ground surface show the air dose rate by the same colors as those in Fig. 2. Land surface is painted based on the terrain height in the ranges of 0–520 (brown) and > 520 m (white).

Movie 2 Same as Supplementary movie 1, but this is the view from the southeast to northwest direction.

FIGURE CAPTIONS

Figure 1.

Observed ground-level air dose rates in Fukushima prefecture by (a) aerial measurements (MEXT and DOE, 2011, reproduced from the authors) and (b) monitoring posts (Fukushima prefecture, 2011a and b). Words in parentheses in (b) show the direction of the locations from FNPP1.

Figure 2.

Topography and simulation domain size of (a) Domain 1 and (b) 3 in MM5 and GEARN. Plots with labels in (b) show the environmental data used to reproduce the meteorological fields and radiological events by WSPEEDI-II. Other plots without labels represent the monitoring posts for comparisons in spatial patterns of air dose rate between observations and calculations by GEARN.

Figure 3.

Comparisons between MM5 calculations with/without nudging (lines) and observations (circles) for wind direction and speed at the surface weather stations located at the northwest (NW) and west (W) directions from FNPP1.

Figure 4.

Comparisons between MM5 calculations with/without nudging (lines) and observations (black lines with dots) for precipitation at the surface weather stations located at the northwest (NW), west (W), west-northwest (WNW), and north (N) directions from FNPP1.

Figure 5.

Temporal changes in (a) wind direction and (b) speed in observations (circles) and MM5 calculations (lines) at FNPP1 and FNPP2.

Figure 6.

Procedure for reconstruction of atmospheric dispersion of radionuclides in Fukushima Daiichi nuclear reactor accident using Worldwide Version of System for Prediction of Environmental Emergency Dose Information (WSPEEDI-II).

Figure 7.

Temporal changes of calculated (lines) and observed (circles) air dose rates at monitoring posts located at the northwest (NW), west (W), west-northwest (WNW), and north (N) directions from FNPP1.

Figure 8.

Simulated spatial distributions of air dose rate (right panels), concentration of ^{131}I, rainfall intensity (shaded areas), and surface wind (vectors) (left_panels) at (a)-(b) 9, (c)-(d) 12, and (e)-(f) 15 JST on March 15, 2011. Values beside circles in right panels represent observed air dose rates at monitoring posts.

Figure 9.

Simulated spatial distributions of air dose rate (right panels), concentration of ^{131}I, rainfall intensity (shaded areas), and surface wind (vectors) (left panels) (a)-(b) 18 and (c)-(d) 21 JST on March 15 and (e)-(f) 9 JST on March 16, 2011 (continued from Fig. 8). Values beside circles in right panels represent observed air dose rates at monitoring posts.

Figure 10.

Spatial distributions of (a) calculated dry and (b) wet deposition and (c) precipitation accumulated from 0 to 21 JST on March 15, 2011.

FIGURE 1

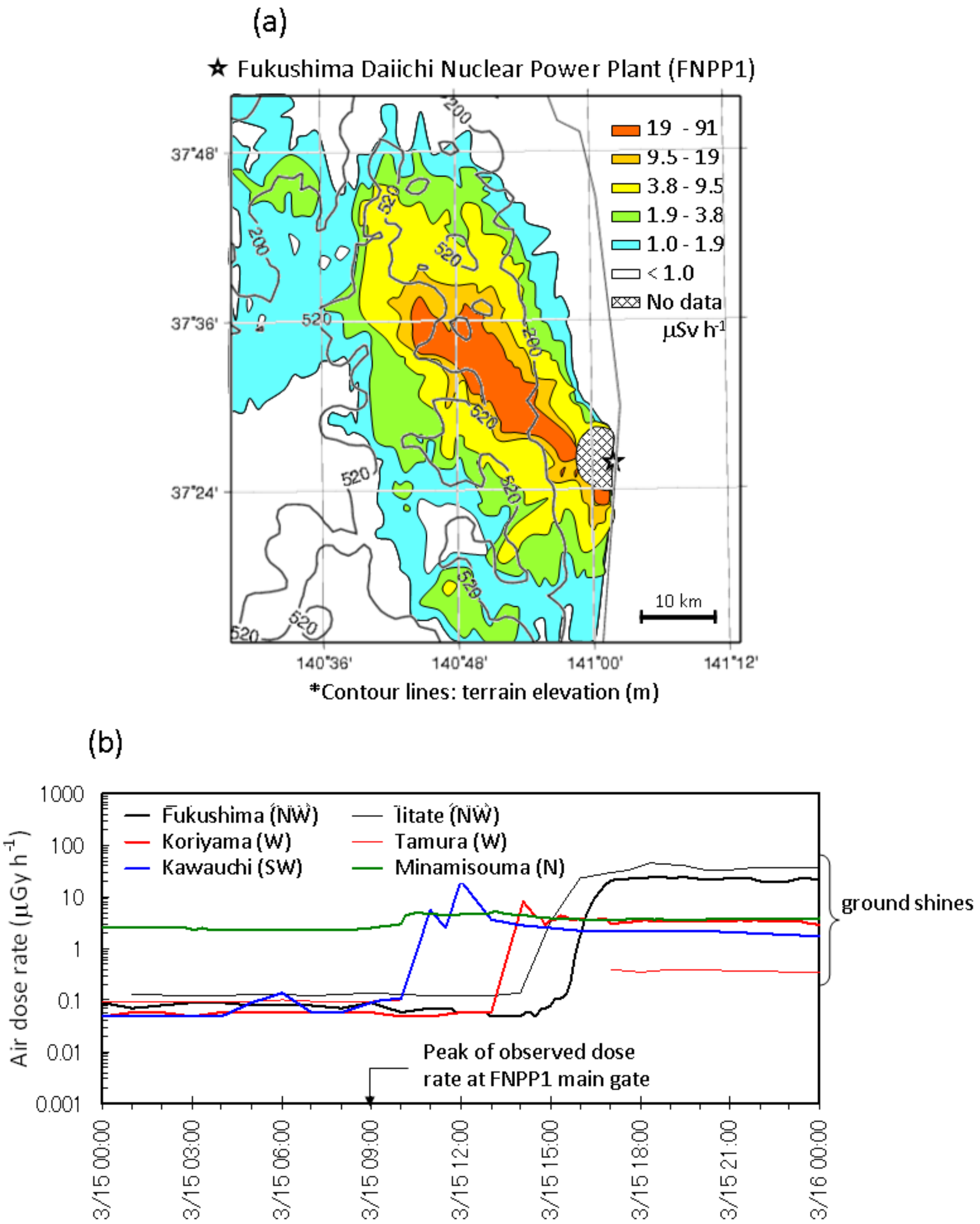

(a)
★ Fukushima Daiichi Nuclear Power Plant (FNPP1)
19 - 91
9.5 - 19
3.8 - 9.5
1.9 - 3.8
1.0 - 1.9
< 1.0
No data
μSv h⁻¹
37°48'
37°36'
37°24'
140°36'
140°48'
141°00'
141°12'
10 km
200
520
*Contour lines: terrain elevation (m)
(b)
Air dose rate (μGy h⁻¹)
1000
100
10
1
0.1
0.01
0.001
Fukushima (NW)
Koriyama (W)
Kawauchi (SW)
Iitate (NW)
Tamura (W)
Minamisouma (N)
ground shines
Peak of observed dose rate at FNPP1 main gate
3/15 00:00
3/15 03:00
3/15 06:00
3/15 09:00
3/15 12:00
3/15 15:00
3/15 18:00
3/15 21:00
3/16 00:00

FIGURE 2

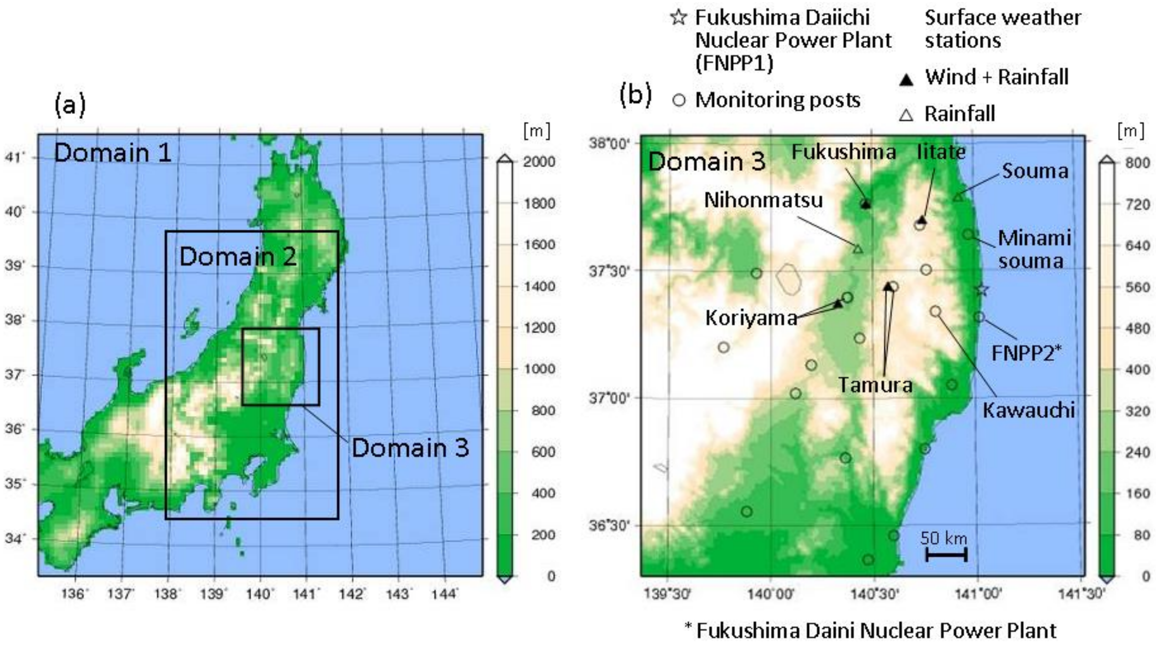

(a)
Domain 1
Domain 2
Domain 3
[m]
2000
1800
1600
1400
1200
1000
800
600
400
200
0
41°
40°
39°
38°
37°
36°
35°
34°
136°
137°
138°
139°
140°
141°
142°
143°
144°
(b)
☆ Fukushima Daiichi Nuclear Power Plant (FNPP1)
○ Monitoring posts
Surface weather stations
▲ Wind + Rainfall
△ Rainfall
Domain 3
Fukushima
Iitate
Souma
Nihonmatsu
Minami souma
Koriyama
FNPP2*
Tamura
Kawauchi
50 km
38°00'
37°30'
37°00'
36°30'
139°30'
140°00'
140°30'
141°00'
141°30'
[m]
800
720
640
560
480
400
320
240
160
80
0
* Fukushima Daini Nuclear Power Plant

FIGURE 3

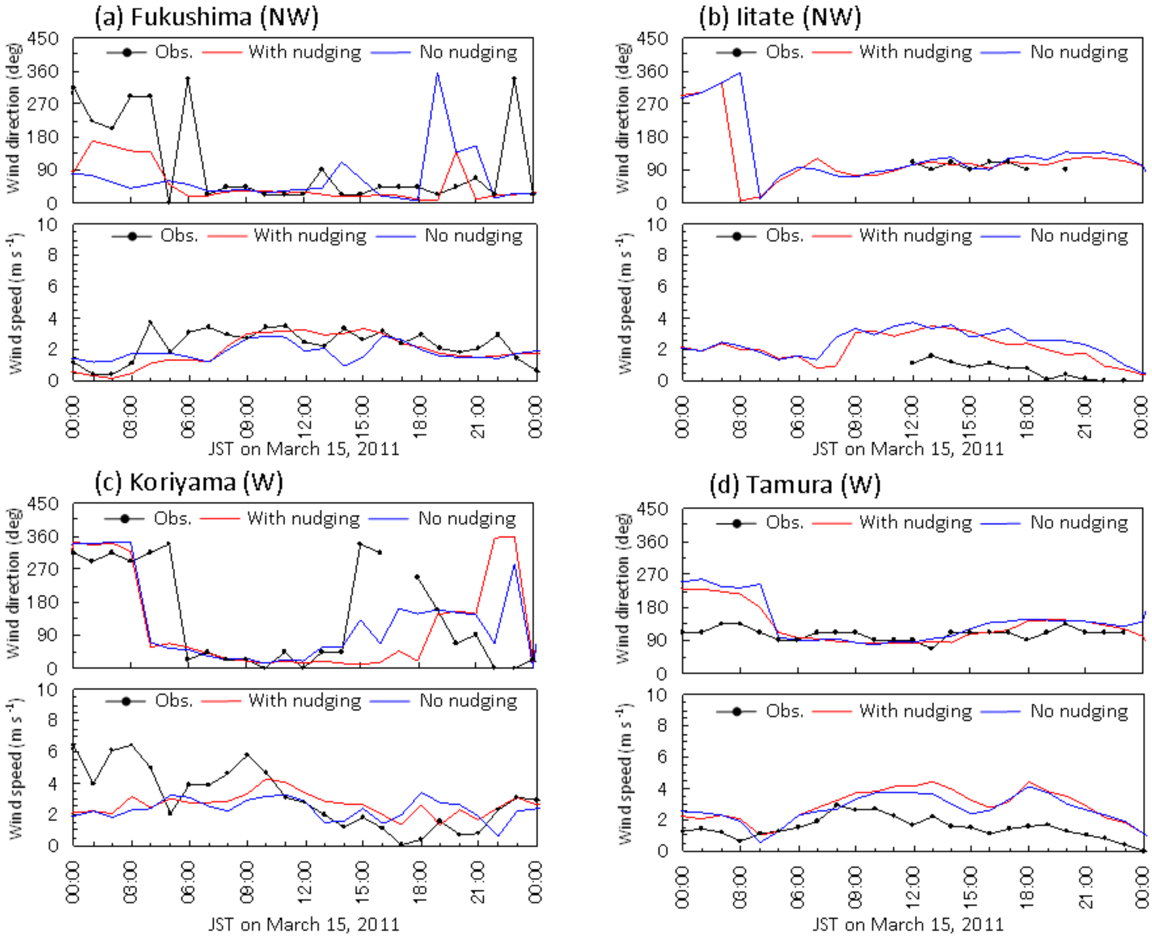
(a) Fukushima (NW)
(b) Iitate (NW)
(c) Koriyama (W)
(d) Tamura (W)
Obs.
With nudging
No nudging
Wind direction (deg)
Wind speed (m s-1)
JST on March 15, 2011

FIGURE 4

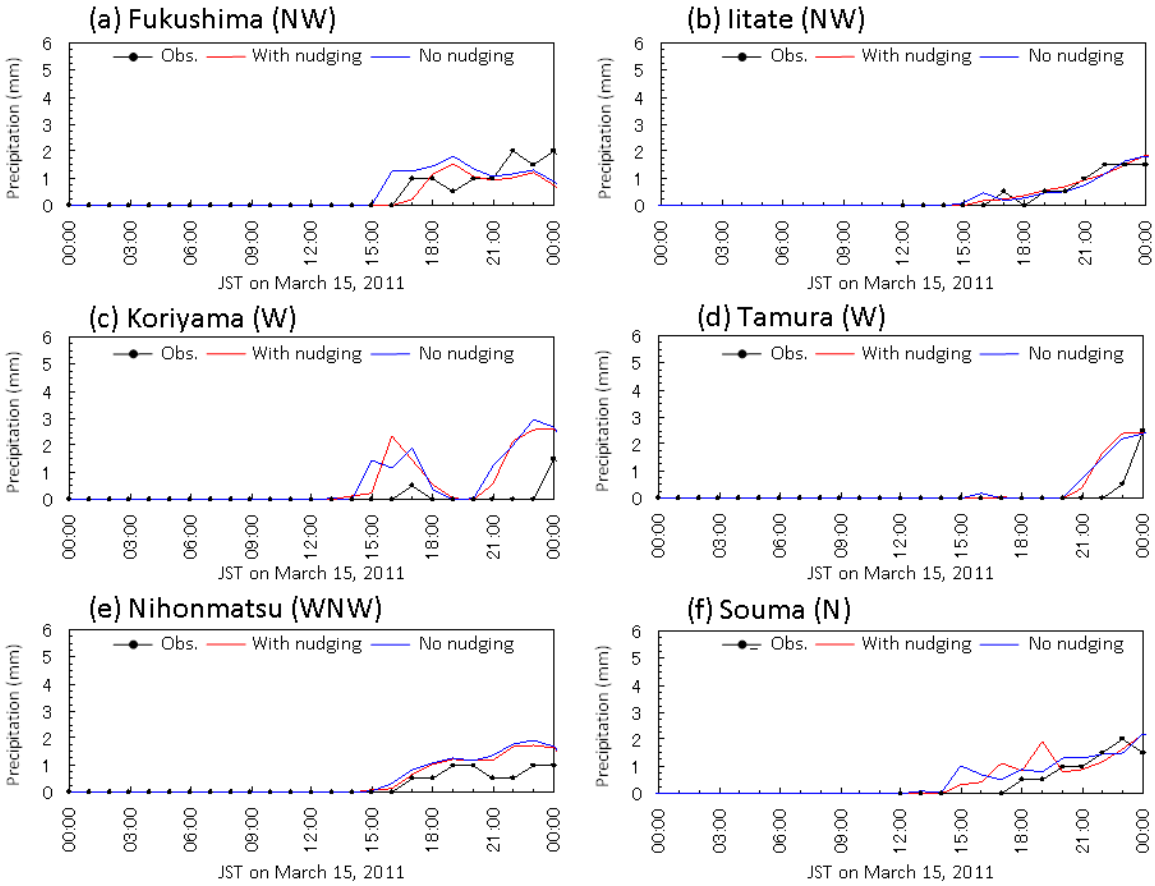
(a) Fukushima (NW)
(b) Iitate (NW)
(c) Koriyama (W)
(d) Tamura (W)
(e) Nihonmatsu (WNW)
(f) Souma (N)
Obs.
With nudging
No nudging
Precipitation (mm)
JST on March 15, 2011
00:00
03:00
06:00
09:00
12:00
15:00
18:00
21:00
00:00

FIGURE 5

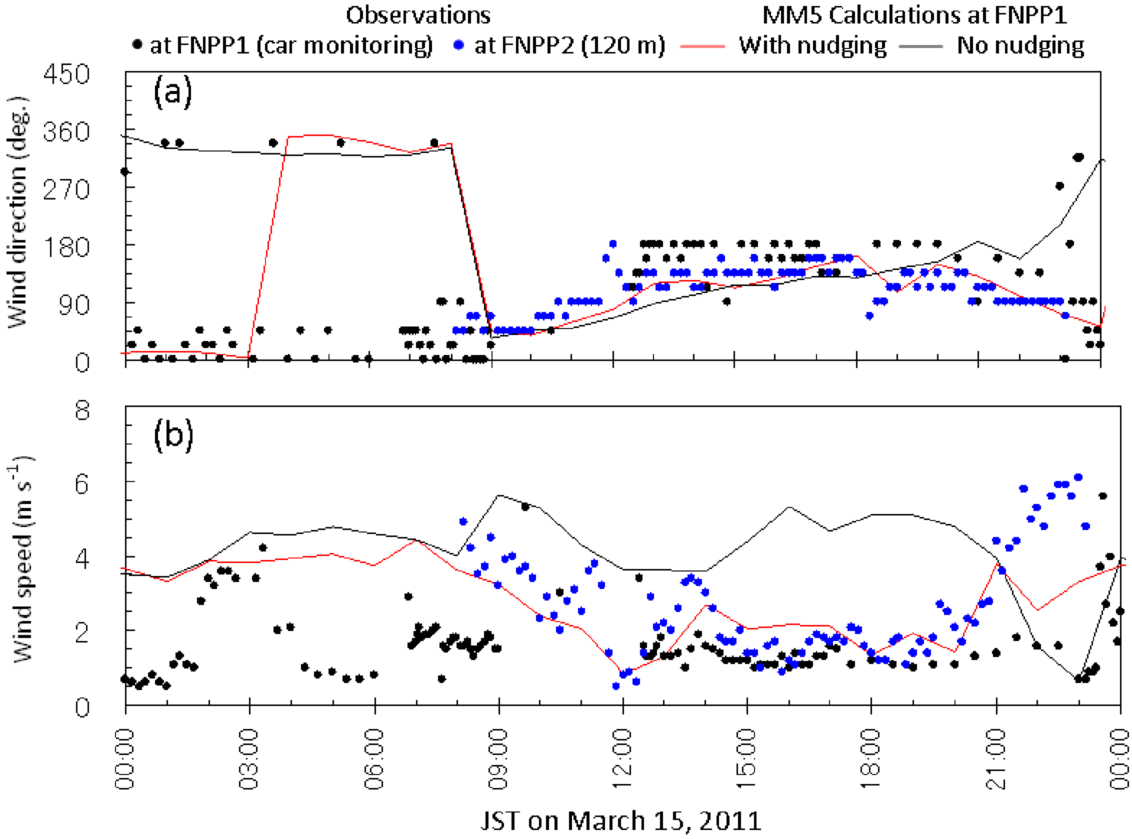
Observations
MM5 Calculations at FNPP1
at FNPP1 (car monitoring)
at FNPP2 (120 m)
With nudging
No nudging
(a)
Wind direction (deg.)
450
360
270
180
90
0
(b)
Wind speed (m s-1)
8
6
4
2
0
00:00
03:00
06:00
09:00
12:00
15:00
18:00
21:00
00:00
JST on March 15, 2011

FIGURE 6

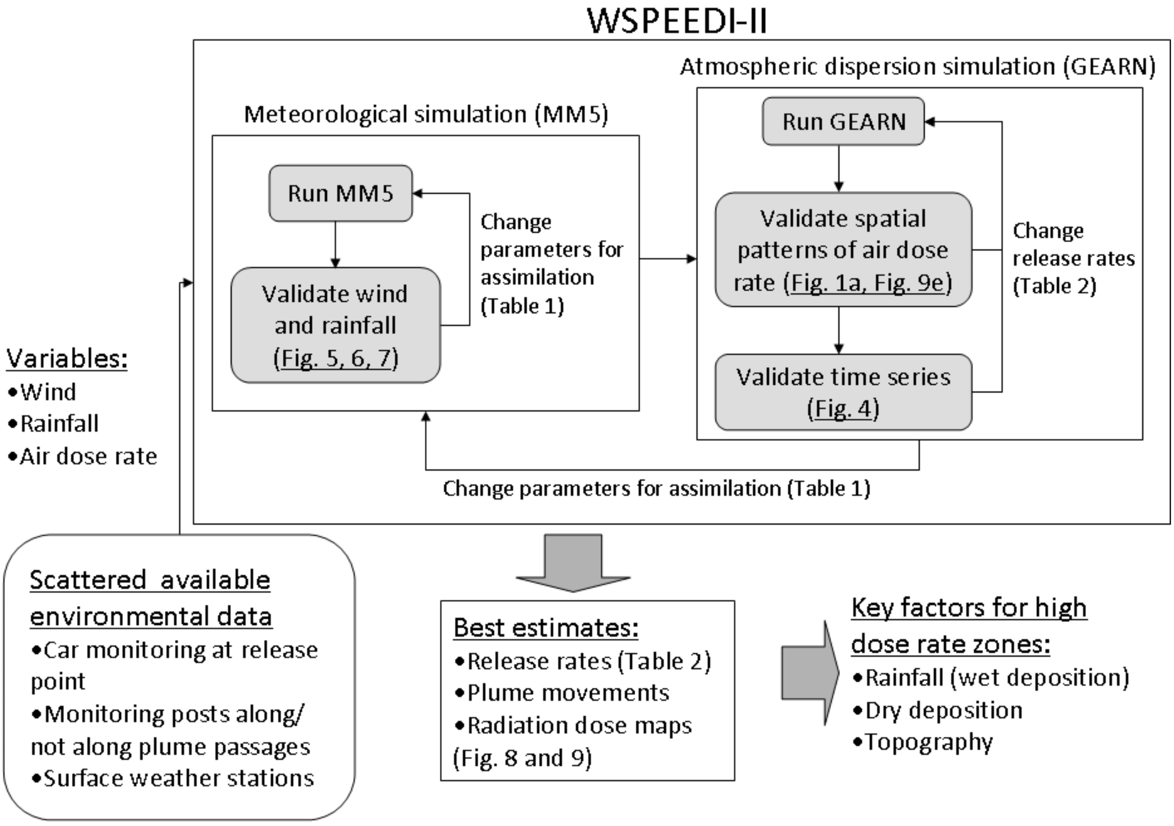
WSPEEDI-II
Atmospheric dispersion simulation (GEARN)
Meteorological simulation (MM5)
Run MM5
Validate wind and rainfall (Fig. 5, 6, 7)
Change parameters for assimilation (Table 1)
Run GEARN
Validate spatial patterns of air dose rate (Fig. 1a, Fig. 9e)
Change release rates (Table 2)
Validate time series (Fig. 4)
Change parameters for assimilation (Table 1)
Variables:
•Wind
•Rainfall
•Air dose rate
Scattered available environmental data
•Car monitoring at release point
•Monitoring posts along/ not along plume passages
•Surface weather stations
Best estimates:
•Release rates (Table 2)
•Plume movements
•Radiation dose maps (Fig. 8 and 9)
Key factors for high dose rate zones:
•Rainfall (wet deposition)
•Dry deposition
•Topography

FIGURE 7

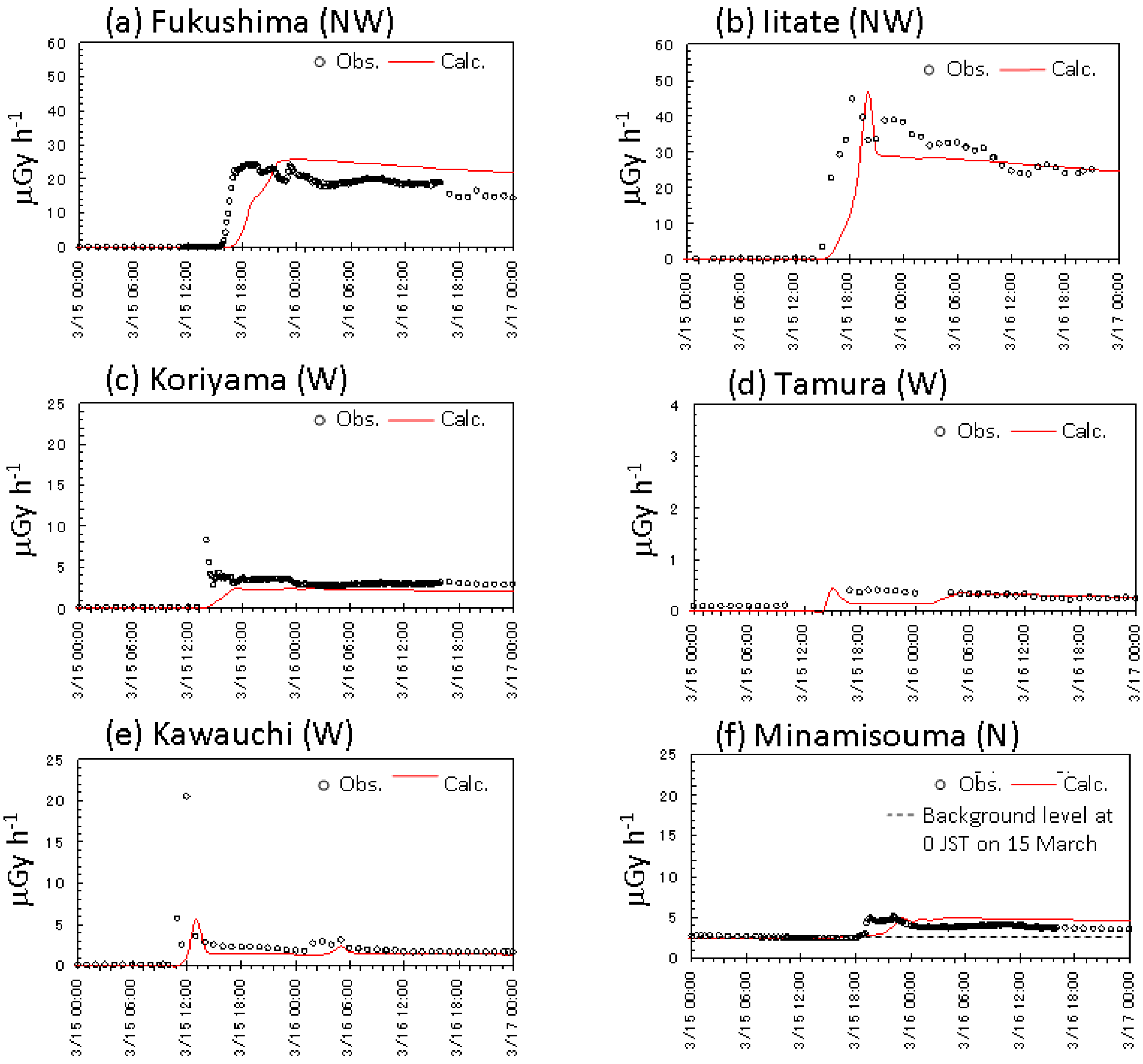

(a) Fukushima (NW)
(b) Iitate (NW)
(c) Koriyama (W)
(d) Tamura (W)
(e) Kawauchi (W)
(f) Minamisouma (N)
Obs.
Calc.
Background level at 0 JST on 15 March
µGy h-1
3/15 00:00
3/15 06:00
3/15 12:00
3/15 18:00
3/16 00:00
3/16 06:00
3/16 12:00
3/16 18:00
3/17 00:00

FIGURE 8

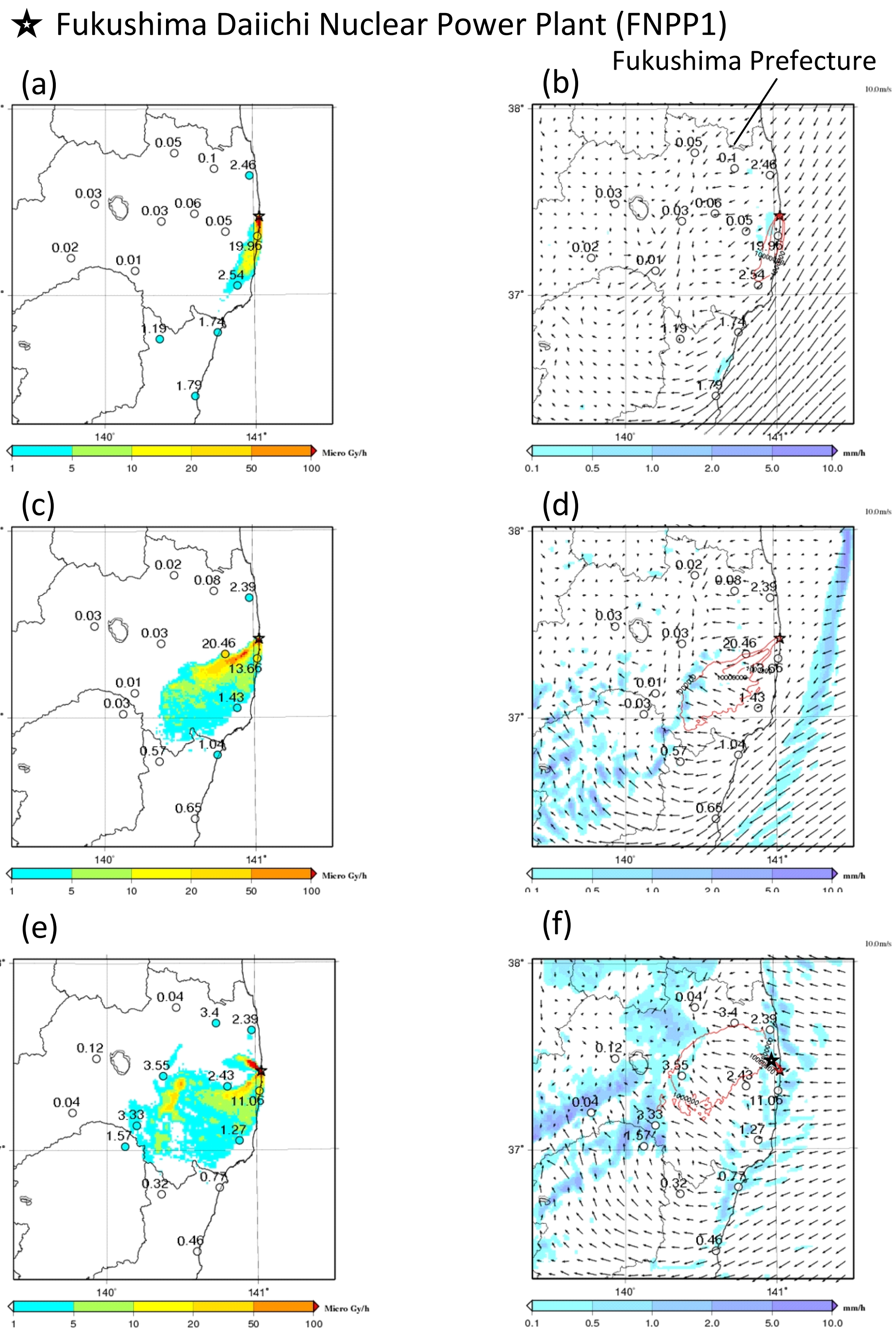
★ Fukushima Daiichi Nuclear Power Plant (FNPP1)
Fukushima Prefecture
(a)
(b)
(c)
(d)
(e)
(f)
38°
37°
140°
141°
Micro Gy/h
1 5 10 20 50 100
mm/h
0.1 0.5 1.0 2.0 5.0 10.0
10.0m/s

FIGURE 9

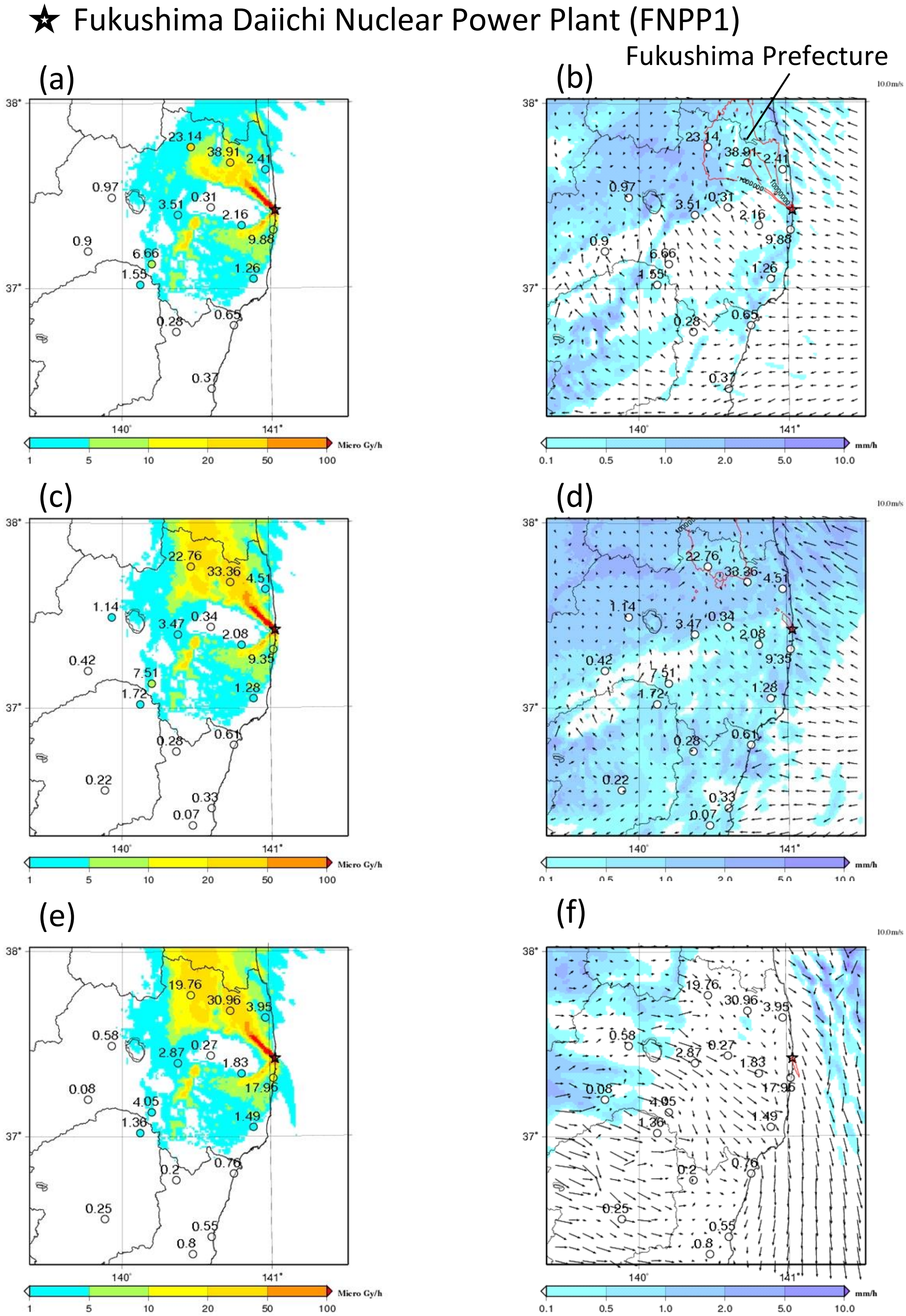

★ Fukushima Daiichi Nuclear Power Plant (FNPP1)
Fukushima Prefecture
(a)
(b)
(c)
(d)
(e)
(f)
Micro Gy/h
mm/h

FIGURE 10

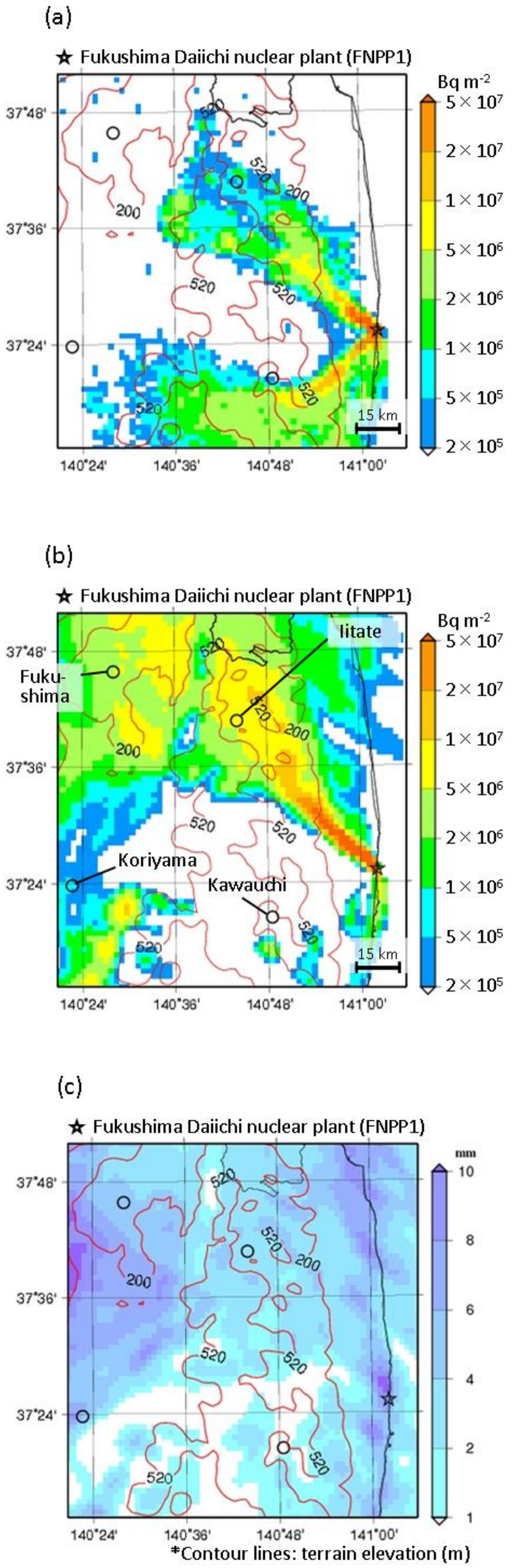
(a)
★ Fukushima Daiichi nuclear plant (FNPP1)
Bq m-2
5 × 10^7
2 × 10^7
1 × 10^7
5 × 10^6
2 × 10^6
1 × 10^6
5 × 10^5
2 × 10^5
15 km
37°48'
37°36'
37°24'
140°24'
140°36'
140°48'
141°00'
(b)
★ Fukushima Daiichi nuclear plant (FNPP1)
Iitate
Fuku-
shima
Koriyama
Kawauchi
(c)
★ Fukushima Daiichi nuclear plant (FNPP1)
mm
10
8
6
4
2
1
*Contour lines: terrain elevation (m)

TABLE CAPTIONS

Table 1.

Simulation settings for atmospheric dynamic model (MM5). Parameters of analysis and observation nudging are optimized to match calculations to observations in meteorological data around FNPP1 (see Fig. 3).

Table 2.

Simulation settings for atmospheric dispersion model (GEARN). Parameters of release rates are optimized to match calculations to observations in air dose rate around FNPP1 (see Fig. 3).

Table 1

	Domain 1	Domain 2	Domain 3
Simulation period	15 JST March 14 – 0 JST March 17, 2011		
Horizontal grid cell	100×100	190×130	190×190
Spatial resolutions	9 km	3 km	1 km
Time step	18 sec.	6 sec.	3 sec.
Vertical levels	31 sigma levels[1] from surface to 100 hPa		
Nesting option	Two-way nested		
Boundary and initial conditions	MSM[2] (0.1°x 0.125° for atmosphere, 0.05°x 0.0625° for the surface layer)		
3D/surface analysis nudging	Utilized with data at FNPP1 (surface), FNPP2 (120 m), and all available surface weather station		
Nudging coefficient (best estimate)	2.5×10^{-4} for wind and temperature and 1.0×10^{-5} for humidity		
Radius of influence (best estimate)	20 km for 3D and 40 km for surface		
Observation nudging	Utilized with data at FNPP1 (surface) and FNPP2 (120 m)		
Nudging coefficient (best estimate)	2.0×10^{-3} for horizontal wind speed		
Radius of influence (best estimate)	40 km		
Physical parameterizations			
Cumulus	Grell		
Cloud microphysics	Schultz microphysics		
Radiation	Cloud-radiation		
Planetary boundary layer	Eta PBL		
Land surface	Five-layer soil model		

[1] Terrain-following half-sigma levels as 1.0, 0.9974, 0.9945, 0.9917, 0.9863, 0.9727, 0.9592, 0.9459, 0.9327, 0.9003, 0.8687, 0.8380, 0.8080, 0.7504, 0.6957, 0.6190, 0.5482, 0.4822, 0.4215, 0.3658, 0.3148, 0.2682, 0.2256, 0.1868, 0.1515, 0.1194, 0.9035, 0.6409, 0.4041, 0.1910, and 0.0.

[2] Meso-scale Spectral Model.

Table 2

	MM5 Domain 2	MM5 Domain 3
Simulation period	17 JST March 14 – 0 JST March 17, 2011	
Spatial resolutions	3 km	1 km
Time step	12 s	4 s
Vertical levels	29 levels from surface (with 20 m thickness layer) to 10 km	
Release height	20 m	
Nesting option	Two-way nested	
Radioactivity ratio	^{131}I:(^{132}I+^{132}Te):^{134}Cs:^{137}Cs = 1:2:0.1:0.1	
Release rates (Bq h^{-1}) for ^{131}I on 15 March		
Preliminary estimation (Chino et al. 2011)	0–9 JST: 3.5×10^{14}, 9–15 JST: 1.0×10^{16}, 15–24 JST: 2.1×10^{14}	
Best estimate*	0–7 JST: 1.0×10^{14}, 7–10 JST: 3.0×10^{15}, 10–13 JST: 8.0×10^{13}, 13–17 JST: 4.0×10^{15}, 17–24 JST: 6.0×10^{13}	

* The estimated release rate from 17 to 24 JST on 15 March was extended until 0 JST on 17 March.